

A physical model for palaeosecular variation

P. L. McFadden and M. W. McElhinny^{*} *Research School of Earth Sciences, Australian National University, GPO Box 4, Canberra, ACT 2601, Australia*

Received 1984 March 7; in original form 1983 October 28

Summary. A new model to describe the latitude dependence of the angular dispersion of the palaeomagnetic field (palaeosecular variation) is developed following previous models, but with crucial differences. It is shown that if the probability distribution of virtual geomagnetic poles (VGPs) is circularly symmetric about the rotation axis then the *geometry* of the distribution of field directions is latitude dependent. This has a significant effect on the latitude dependence of dispersion and is accounted for in the model. The dipole and non-dipole parts of the field are not artificially separated but are intimately linked through an observationally determined relation that the time averaged intensity of the non-dipole field is dependent upon the intensity of the dipole field. It is shown that a consequence of this relation is that no knowledge of the probability distribution of the geomagnetic dipole moment is required. This is a fundamental improvement over previous models.

The model provides excellent fits to the palaeodata and, unlike previous models, is not inconsistent with the latitude variation of the non-dipole field dispersion determined from the present field. For the past 5 Ma the point estimate of the VGP dispersion due to dipole wobble is 7.2° and of the VGP dispersion at the equator due to variation in the non-dipole field is 10.6° . This estimate of the dispersion due to variation in the non-dipole field is in excellent agreement with the value predicted from an analysis of the variation in field intensities over the same period. Fits of the model to data from earlier periods indicate that dispersion due to variation in the non-dipole field is essentially independent of the geomagnetic reversal rate while dipole wobble is positively correlated with reversal rate.

1 Introduction

Studies of the geomagnetic secular variation in historic times are made by analysing changes with time that have occurred in various geomagnetic parameters. Such studies have been extended back to 10 000 yr or more by measurements of the magnetic signal preserved in

^{*}Both now at Division of Geophysics, Bureau of Mineral Resources, GPO Box 378, Canberra, ACT 2601, Australia.

slowly deposited lake sediments. Master curves for the changes in declination and inclination with time over the past 10 000 yr are now available for Great Britain (Thompson & Turner 1979) and SE Australia (Barton & McElhinny 1981). Unfortunately, on the longer (geological) time-scale it is not possible to obtain detailed sequential records of the variations in the geomagnetic field at any locality. However, it has long been recognized (Creer, Irving & Nairn 1959; Creer 1962a, b) that the directional dispersion of the palaeofield at a given locality is accessible and provides valuable information regarding the secular variation. Cox (1962) extended the analysis to the corresponding virtual geomagnetic poles (VGPs). Studies of the latitude variation of the angular dispersion of the geomagnetic field, as measured from palaeomagnetic results, are now generally referred to as *palaeosecular variation (PSV)* studies. For a fuller account of the development of PSV studies reference should be made to the review by McElhinny & Merrill (1975).

Models of PSV commonly ascribe the angular dispersion to variation in the non-dipole field, dipole wobble (changes in the orientation of the central dipole, such that on average the dipole axis coincides with the axis of rotation) and variation in the dipole moment (dipole moment is used throughout this paper as the magnitude of the dipole vector). Variations in dipole moment do not contribute a separate source as such but affect the dispersion from variations in the non-dipole field (however, see Section 3). Consequently the dispersion ascribed to variations in the non-dipole field includes any effects from variation in the dipole moment. Even though it is physically unrealistic to separate the dipole and non-dipole components it is an intuitively appealing approach because of conceptual simplicity and, provided the mathematics of the model does not require an actual separation or different sources, it is quite acceptable. Using the nomenclature of Irving (1964) the models which have been suggested are as follows.

(1) Model A (Irving & Ward 1964) considers an axial geocentric dipole of fixed moment perturbed by a central dipole of fixed magnitude but random direction.

(2) Model B (Creer *et al.* 1959; Creer 1962a, b) assumes a wobble of the main dipole which follows a Fisher (1953) distribution. Non-dipole components are not considered.

(3) Model C (Cox 1962) combines dipole wobble with non-dipole components based on parameters derived from the present field.

(4) Model D (Cox 1970) supersedes model C and again combines dipole wobble with non-dipole components but uses generalized statistical models to specify the non-dipole field.

(5) Model E (Baag & Helsley 1974) proposes that the sources of dispersion are not independent and attempts to account for the observed variations in dispersion using a correlation function.

(6) Model M (McElhinny & Merrill 1975) follows model D but uses a different latitudinal variation for the average intensity of the non-dipole field components. Contributions to the non-dipole dispersion arise from two sources, one producing components having symmetrical field direction distributions and the other components having symmetrical VGP distributions. Unfortunately an error in their analysis has subsequently shown the model to be incorrect (Harrison 1980).

Each of the above models has been singularly unsuccessful in matching the latitude variation of the angular dispersion determined from the present geomagnetic field. Harrison (1980) tried to circumvent this problem by modifying the equations in model M to obtain a match to the present field variation (essentially a curve fitting process). His resulting equation is, however, physically unrealistic. Models A and B are clearly too simplistic and model C has the implicit assumption that the latitude variation of the present non-dipole

field is characteristic of the time-averaged variation (see Section 2 for discussion). A major problem common to models D, E and M is that they require knowledge of the probability distribution of the average intensity of the non-dipole components and of the dipole moment. Each of these models has used as a probability density for the dipole moment the density implied by Cox's (1968) model of an oscillating dipole moment. It is now known that this probability distribution is incompatible with the observed distribution of virtual dipole moments (VDMs) following the analyses of Kono (1972) and McFadden & McElhinny (1982).

Roy & Wagner (1982) have presented a PSV model based on a pair of unequally sized current loops in the core. This model does have the appeal that there is no artificial separation into dipole and non-dipole parts. However, 14 time-dependent parameters are required to specify the pair of loops and estimation of these parameters, together with their time dependence, from palaeosecular variation data is a formidable task. Roy & Wagner use a fit, presented by Zidarov & Petrova (1979), to the well-specified 1950 field and allowed time variations only through orientation of the loops. The model is entirely deterministic and so a fit to the parameters and their evolution would require accurate dating of PSV data with extensive global coverage at each (precise) age. Present PSV data represent, at best, samples at random times and random positions. For the foreseeable future therefore it would be inappropriate to attempt to fit a deterministic model to PSV data. Instead the stochastic sampling of the deterministic processes should be recognized and attempts made to fit statistical models.

This paper thus aims to produce a statistical model for the latitude variation of angular dispersion without the inconsistencies of previous models. A model is required which: (a) is not inconsistent with the latitude variation in the angular dispersion obtained from the present field, (b) retains an intimate link between the dipole and non-dipole parts of the field and (c) is not inconsistent with our present understanding of the variation in the intensity of the field. Consistent with previous nomenclature, the model is referred to as model F.

2 Model non-uniqueness and the present-day field

McElhinny & Merrill (1975) have previously discussed the fact that, given a set of PSV data, it is not possible to separate the effects of dipole wobble and non-dipole variation in a unique manner. A brief resumé of their argument is presented here for completeness.

It is now well-known that the angular dispersion of geomagnetic field directions decreases with latitude. This is true both for the dispersion caused by dipole wobble and the dispersion caused by variation in the non-dipole components. However, if the field directions are transformed to virtual geomagnetic poles (VGPs) then the dispersion caused by dipole wobble is independent of latitude and the dispersion caused by variation in the non-dipole components increases with latitude, the resulting overall dispersion therefore also increases with latitude. The latitude independence of the dispersion from dipole wobble in the VGP frame of reference makes this the natural frame of reference for estimation of model parameters. Hence the model for dispersion from the non-dipole field is developed in the direction frame of reference and then transformed to the VGP frame of reference for addition of the dipole wobble dispersion and parameter estimation.

The overall angular dispersion of VGPs, S , is usually written as

$$S^2 = S_D^2 + S_N^2 W^2(\lambda) \quad (1)$$

(e.g. see review by McElhinny & Merrill 1975) where S_D is the angular dispersion of VGPs caused by dipole wobble, λ is the latitude, S_N is the angular dispersion of VGPs at $\lambda = 0$

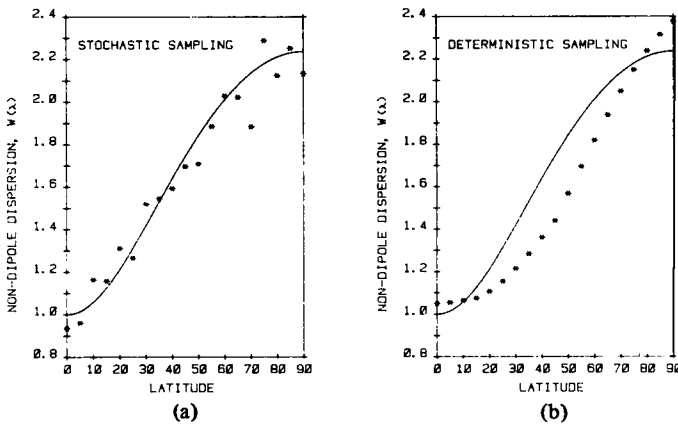


Figure 1. The solid curve represents the actual time-averaged latitude variation. (a) Variation about this curve from independent observations (i.e. the sampling is carried out on a stochastic time-scale). (b) Systematic variation from the time-averaged curve obtained by sampling at different latitudes but at a fixed time (i.e. the sampling is carried out on a deterministic time-scale). Each observation in (a) is therefore a *single* point from a deterministic curve such as the dotted curve in (b) but each one is drawn from a different, independent curve.

caused by variation in the non-dipole components and $W(\lambda)$ is the latitude variation in the non-dipole dispersion with, by definition, $W(0) = 1$.

Consider now a set of palaeosecular variation data from which the dispersion of VGPs is known as a function of λ the value at the equator ($\lambda = 0^\circ$) being 13° and at the pole ($\lambda = 90^\circ$) being 19° . If it is assumed that the dipole wobble gives $S_D = 5^\circ$ then $S_N W(0) = 12^\circ$ and $S_N W(90) = 18.3^\circ$. Consequently the latitude variation $W(90)/W(0)$ for the non-dipole dispersion is 1.53. However, if it is assumed that the dipole wobble gives $S_D = 12.5^\circ$ then $S_N W(0) = 3.57^\circ$ and $S_N W(90) = 14.31^\circ$, giving the latitude variation $W(90)/W(0) = 4.01$. Thus a very different latitude variation is required depending on the amount of dipole wobble. Furthermore, the *shape* of the latitude variation will also alter. Consequently many different models, all predicting different functions $W(\lambda)$, can be made to fit the palaeosecular variation data by adjusting the amount of dipole wobble. The only way to overcome this modelling non-uniqueness is to require that the model predict a $W(\lambda)$ which is consistent with the latitude variation of the present-day non-dipole field. However, there is also a slight problem associated with this approach, as is shown below.

When angular dispersions are obtained from a set of palaeomagnetic measurements, then it can be assumed that individual observations, both at the same and different latitudes, will tend to be separated enough in time that each observation is independent. Essentially therefore sampling is being carried out on a stochastic time-scale. The observations can thus be expected to group around the correct curve as shown in Fig. 1(a). With the present-day non-dipole field the situation is somewhat different. By rotating the present non-dipole field around lines of latitude, an estimate of the latitude variation of the angular dispersion, based entirely on the present field, may be obtained. However, because a real field has been used and rotated, the angular dispersions obtained for different latitudes are not independent of each other. These dispersions are then not observations on a stochastic time-scale but are observations on a deterministic time-scale. From the equator to the pole there appears to be about one 'wavelength' of non-dipole features. It is thus unlikely that more than three of the observations from equator to pole are independent. This means that it can be expected that the *shape* of the curve derived from the present non-dipole field would differ from the

shape of the curve derived from the time-averaged field (Fig. 1b). However, it can still be expected that the ratio $W(90)/W(0)$ will be similar for the two fields, so that much of the non-uniqueness can be removed by requiring that this be the case. However, it is still to be expected that the *shape* of the two curves will vary in a deterministic manner (Fig. 1b).

3 Model assumptions

Cox (1970) points out that low latitude present-day field directions are not symmetric but their corresponding VGP positions are approximately symmetric. It seems reasonable therefore for modelling purposes to assume that the VGPs, rather than the field directions, exhibit symmetry. As the basic structure for the model, with regard to dispersion due to non-dipole components, it has thus been assumed that the field at a given point and given time may be considered as resulting from a dipole \mathbf{M}_r which is itself the resultant of the actual dipole \mathbf{M} perturbed by another dipole \mathbf{m} (representing the non-dipole components), as shown in Fig. 2. Changes in the direction of \mathbf{M} are then associated with dipole wobble and the dipole moment, M , is just the length of this vector. If the dipole moment is sampled on a stochastic time-scale the resulting distribution of M will have some probability density,

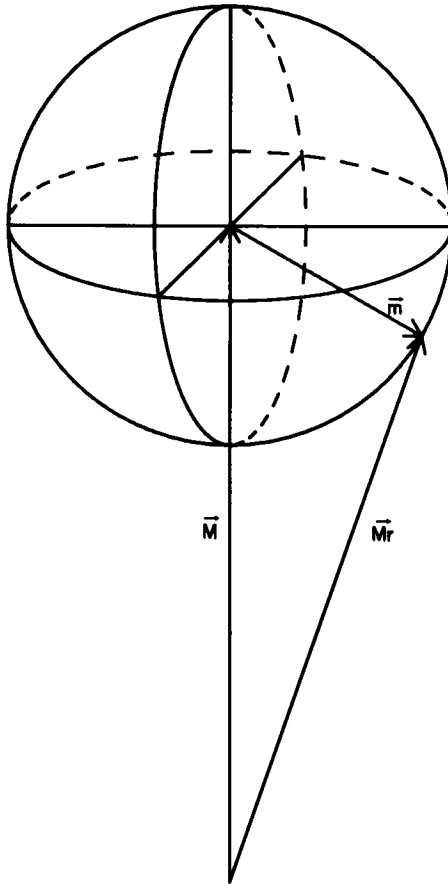


Figure 2. Geometry of vectors assumed for the VGP frame of reference. \mathbf{M} represents the dipole vector, \mathbf{m} the non-dipole vector and \mathbf{M}_r the resultant.

denoted by $P_M(M)$. Variations in the non-dipole components are represented by variations in the length and direction of \mathbf{m} . The distribution of \mathbf{m} will depend on both longitude and latitude, λ , but in the time-averaged sense it will depend only on λ . The assumption of spherical symmetry in the VGPs requires that \mathbf{m} be uniformly distributed in direction so that for a given m (the length of \mathbf{m}) and M , the tip of the vector \mathbf{M}_R will lie on the surface of a sphere (Fig. 2). The non-dipole components change over periods from 10 to 10^3 yr while the dipole changes over periods of about 10^4 yr (Cox & Doell 1964). Because of this difference in time constants there is the possibility that the distribution of m depends on the value of M and, as shown below, there is evidence to suggest this is so. Consequently a density, $p_m(m|M; \lambda)$, is assumed of m conditional upon given M with a dependence on λ .

For a dipole of given moment M aligned along the spin axis let the intensity be F_0 at the equator. At some latitude λ the intensity, F , from the dipole field will then be given by

$$F = F_0 \sqrt{1 + 3 \sin^2 \lambda}. \quad (2)$$

Consequently in the case of field directions it may be considered that the dipole vector \mathbf{M} has been mapped into a field vector \mathbf{F} and the density $P_M(M)$ will have been mapped into some density $P_F(F; \lambda)$, the dependence on λ arising from equation (2). For a given M and λ the vector \mathbf{m} will map into some field vector \mathbf{v} (Fig. 3) and the resultant vector \mathbf{M}_R will map into the resultant field vector \mathbf{F}_R . However, unlike the tip of \mathbf{M}_R , for a given m , M and λ , the tip of \mathbf{F}_R is not distributed on the surface of a sphere. Instead it is distributed over a surface which is more like an ellipsoid of revolution with axes α , β and γ ($\alpha \neq \beta \neq \gamma$) (Fig. 3). If f^2 is the average of v^2 over this surface (i.e. for given m , M and λ) then, as M maps into F , so also m maps into f and $p_m(m|M; \lambda)$ maps into the density $p_f(f|F; \lambda)$.

On the basis of archaeomagnetic results McElhinny & Senanayake (1982) suggested that, to first order, the average intensity of the non-dipole components has been proportional to the dipole field. This was confirmed by a statistical analysis presented by McFadden & McElhinny (1982) of VDMs from the past 5 Myr. In their analysis McFadden & McElhinny (1982) showed that an excellent fit to the distribution of VDMs is obtained by assuming that for a given dipole moment (or dipole field intensity F) the variance in observed VDMs consequent upon non-dipole components is proportional to the square of the dipole moment (or F^2). This suggests that to first order

$$\int_f f^2 p_f(f|F; \lambda) df = \langle f^2 | F \rangle = k^2 F^2 \quad (3)$$

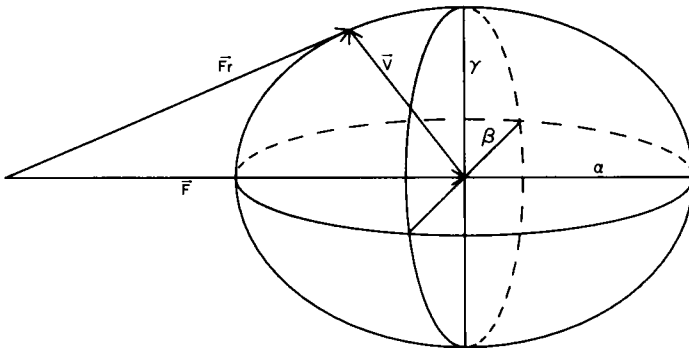


Figure 3. Geometry of field direction vectors at observation point. The vectors \mathbf{M} , \mathbf{m} and \mathbf{M}_R from the VGP frame of reference (Fig. 2) map into the vectors \mathbf{F} , \mathbf{v} and \mathbf{F}_R respectively. A spherical surface in the VGP frame of reference maps into a non-spherical surface with axis lengths α , β and γ (see text).

where the integration is over all possible f , $\langle f^2 | F \rangle$ is the expectation of f^2 conditional upon given F and k is a constant. This equation is equivalent to stating that at any latitude the time-averaged energy density in the non-dipole field is a constant proportion of the energy density in the dipole field and this linearity is assumed throughout the analysis.

As is shown later the angular variance in directions from variations in the non-dipole field is proportional to the expectation of (f^2/F^2) . Therefore, from equation (3), as F varies so does the distribution of f so that the dispersion due to variations in the non-dipole field remains constant. Consequently, in the present model, variations in the dipole moment do not affect the dispersion. Hence, even if the dipole moment, M , is correlated with the direction of \mathbf{M} this does not imply any correlation between dispersion from dipole wobble and dispersion from variations in non-dipole components. However, as dipole wobble occurs the magnetic latitude at a given geographic latitude will vary and this does imply a correlation of the two effects through λ . However, this will be a second-order effect and so for this model it is assumed that the resulting covariance between S_D and S_N is negligible. Hence it is assumed throughout the analysis that equation (1) is valid.

In the next section the model for palaeosecular variation is developed solely from the above assumptions. It is rather surprising that these assumptions are sufficient but, as will be shown, there is no need to make any assumptions regarding the distributions $P_F(F; \lambda)$ and $p_f(f|F; \lambda)$ apart from the relation of equation (3).

4 Development of model F

As the latitude, λ , of observation varies so do the *relative* lengths of the axes α , β and γ in Fig. 3. Consequently, for a given ratio (f/F) , the angular dispersion observed will be latitude-dependent. This mapping is difficult to perform analytically and so it has been done numerically. If $\alpha = \beta = \gamma = f \ll F$ then it is a trivial matter to show that

$$\delta_d^2 = \frac{2}{3} \frac{f^2}{F^2} \tag{4}$$

where δ_d^2 is the angular variance of field directions with δ_d in radians. Thus it can be expected that for the actual mapping, for a given f and F , the function will be similar to this but with a term describing the latitude variation and also terms describing the correction for finite f . It has been found by the numerical process that an extremely close fit to the actual mapping is provided by the function

$$\delta_d^2(\lambda) = \frac{2}{3} \frac{1 + a \exp(-b\lambda^2)}{\sqrt{1 + 3 \sin^2 \lambda}} \frac{f^2}{F^2} = G(\lambda) \frac{f^2}{F^2} . \tag{5}$$

The term $\sqrt{1 + 3 \sin^2 \lambda}$ accounts for the latitude variation in the *relative* lengths of the axes α , β and γ and, strangely enough, this effect has been completely ignored in all previous models. The term $[1 + a \exp(-b\lambda^2)]$ is a correction factor for finite f and so both a and b depend on the angular variance of field directions at the equator, i.e. $\delta_d^2(0)$. However, over the range of interest, both a and b vary slowly and their values may be obtained by linear interpolation from Table 1.

As f and F vary the time-averaged angular variance of the field directions, $\sigma_d^2(\lambda)$, must be given by

$$\sigma_d^2(\lambda) = \int_F \int_f \delta_d^2(\lambda) p_f(f|F; \lambda) P_F(F; \lambda) df dF \tag{6}$$

Table 1. Values of a and b as a function of $\delta_d(0)$.

$\delta_d(0)$	a	b
2°	0.2430	10.860x10 ⁻⁴
4°	0.2400	10.664x10 ⁻⁴
6°	0.2349	10.323x10 ⁻⁴
8°	0.2278	9.847x10 ⁻⁴
10°	0.2186	9.238x10 ⁻⁴
12°	0.2073	8.498x10 ⁻⁴
14°	0.1939	7.646x10 ⁻⁴
16°	0.1788	6.629x10 ⁻⁴
18°	0.1615	5.475x10 ⁻⁴
20°	0.1442	4.536x10 ⁻⁴

Note

(1) In this table $\delta_d(0)$ is in degrees and the value of b given assumes that in the equation $[1 + a \exp(-b\lambda^2)]$, λ is in degrees.

(2) The nature of the correction is such that $\sigma_d(0)$ may be substituted for $\delta_d(0)$ and the values of a and b are still sufficiently accurate. See text.

where the integration is over all possible values of f and F . The function $G(\lambda)$ is, through a and b , weakly dependent on the ratio (f/F) and therefore on the density $p_f(f|F; \lambda)$. However, this dependence is dominated by the ratio $(\langle f^2 | F \rangle / F)$ and so if the values of a and b are determined from $\sigma_d^2(0)$ rather than $\delta_d^2(0)$ the function $G(\lambda)$ may be considered as independent of $p_f(f|F; \lambda)$ and only very small errors will be introduced in the correction for finite f . Substitution for $\delta_d^2(\lambda)$ from (5) into (6) then gives

$$\begin{aligned}
 \sigma_d^2(\lambda) &= \int_F \int_f G(\lambda) \frac{f^2}{F^2} p_f(f|F; \lambda) P_F(F; \lambda) df dF \\
 &\cong G(\lambda) \int_F \frac{1}{F^2} P_F(F; \lambda) \left[\int_f f^2 p_f(f|F; \lambda) df \right] dF \\
 &= G(\lambda) \int_F \frac{\langle f^2 | F \rangle}{F^2} P_F(F; \lambda) dF.
 \end{aligned}
 \tag{7}$$

Substitution from (3) then gives

$$\begin{aligned}
 \sigma_d^2(\lambda) &= G(\lambda) \int_F k^2 P_F(F; \lambda) dF \\
 &= k^2 G(\lambda)
 \end{aligned}
 \tag{8}$$

and it should be noted that this result is essentially *independent* of the distribution of *either* f or F , i.e. of $p_f(f|F; \lambda)$ and $p_F(F; \lambda)$. This is a distinct advantage over previous models.

It now remains to transform from the angular variance of field directions, $\sigma_d^2(\lambda)$, to the angular variance of VGPs, $\sigma_p^2(\lambda)$. Denoting the transformation by $H \{ \lambda, \sigma_d^2(\lambda) \}$ where

$$H \{ \lambda, \sigma_d^2(\lambda) \} = \sigma_p^2(\lambda) / \sigma_d^2(\lambda) \tag{9}$$

then

$$\sigma_p^2(\lambda) = k^2 G(\lambda) H \{ \lambda, \sigma_d^2(\lambda) \} . \tag{10}$$

If $\sigma_d^2(\lambda)$ is very small then $H \{ \lambda, \sigma_d^2(\lambda) \}$ is a function only of λ and Cox (1970) has given the transform as

$$H \{ \lambda, \sigma_d^2(\lambda) \rightarrow 0 \} = \frac{2(1 + 3 \sin^2 \lambda)^2}{5 + 3 \sin^2 \lambda} . \tag{11}$$

However, for typical values of $\sigma_d^2(\lambda)$ this relation is not accurate enough and the transformation has to be performed numerically. This has already been done by Cox (1970) and the transformation presented in tabular form (see his table 5). This tabular transformation is reproduced here as Table 2 and interpolation within the table may be performed as a linear interpolation for $\sigma_d^2(\lambda)$ and a non-linear interpolation for λ assuming the functional form of equation (11).

Using the notation of (1), (10) may be rewritten as

$$\begin{aligned} \sigma_p^2(\lambda) &= S_N^2 \frac{G(\lambda) H \{ \lambda, \sigma_d^2(\lambda) \}}{G(0) H \{ 0, \sigma_d^2(0) \}} \\ &= S_N^2 W^2(\lambda) \end{aligned} \tag{12}$$

where

$$S_N^2 = k^2 G(0) H \{ 0, \sigma_d^2(0) \} . \tag{13}$$

Table 2. Transformation function $H \{ \lambda, \sigma_d^2(\lambda) \}$ from angular variance of field directions to angular variance of VGPs as a function of λ and $\sigma_d^2(\lambda)$.

λ	Equation					
	(11)	$\sigma_d^2(\lambda)=0,01$	$\sigma_d^2(\lambda)=0,02$	$\sigma_d^2(\lambda)=0,04$	$\sigma_d^2(\lambda)=0,08$	$\sigma_d^2(\lambda)=0,16$
0°	0.40	0.41	0.42	0.44	0.48	0.54
10°	0.47	0.47	0.48	0.49	0.52	0.57
20°	0.68	0.68	0.67	0.66	0.66	0.68
30°	1.07	1.04	1.02	0.99	0.94	0.89
40°	1.61	1.57	1.54	1.48	1.37	1.22
50°	2.25	2.21	2.17	2.09	1.94	1.69
60°	2.91	2.87	2.83	2.73	2.56	2.23
70°	3.48	3.44	3.39	3.30	3.11	2.74
80°	3.86	3.83	3.78	3.69	3.50	3.11
90°	4.00	3.97	3.92	3.83	3.64	3.25

Note

In this table λ is in degrees but $\sigma_d(\lambda)$ is in radians.

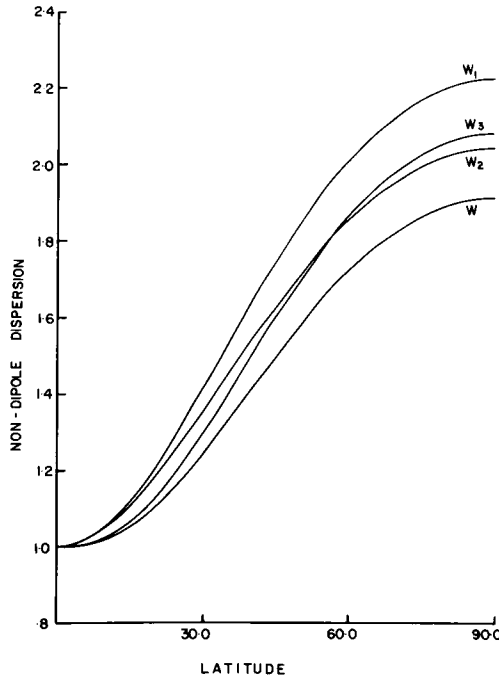


Figure 4. Non-dipole latitude variation, $W(\lambda)$, predicted by model F with an assumed value of $\sigma_d(0) = 12.4^\circ$. $W_1(\lambda)$, $W_2(\lambda)$ and $W_3(\lambda)$ indicate the effects of ignoring different aspects of finite non-dipole dispersion.

The latitude variation, $W(\lambda)$, of the non-dipole dispersion according to this model is shown in Fig. 4 for an assumed value of $\sigma_d(0) = 12.4^\circ$. For comparison purposes approximations to $W(\lambda)$ have also been plotted in the same diagram. $W_1(\lambda)$ assumes that in (5) $a = 0$ and uses (11) for the transformation to the poles. Hence the corrections for finite dispersion have been ignored both in the dispersion of field directions and in the transformation to the poles. $W_2(\lambda)$ uses the correct values for a and b in (5) but still uses (11) for transformation to the poles. Hence the correction for finite dispersion has been ignored only in the transformation to the poles. $W_3(\lambda)$ again assumes $a = 0$ in (5) but uses the correct transformation to the poles. Hence the correction for finite dispersion has been ignored only in the dispersion of field directions.

5 Estimation of model parameters

From (1),

$$S^2 = S_D^2 + S_N^2 W^2(\lambda), \quad (1)$$

a plot of the overall angular variance S^2 against the latitude variation $W^2(\lambda)$ will be linear. Thus, least squares linear regression techniques may be used to estimate the parameters S_D and S_N . Because of the nature of sampling, the observations at different latitudes have different precisions and therefore a weighted least squares regression has been used.

The relationship is such that the parameters actually estimated are S_D^2 and S_N^2 and simply taking the square root of the estimates for these parameters will give biased estimates for the parameters S_D and S_N . Furthermore, $W^2(\lambda)$ depends implicitly upon $\sigma_d^2(0)$ and

therefore on S_N^2 , one of the parameters to be estimated. Hence an iterative least squares regression, on $\sigma_d^2(0)$ or equivalently S_N^2 , has to be performed. This lack of independence means that the usual estimates of error in the least squares fit will be at best rough estimates of the actual error involved. To overcome these problems a jack-knife technique (see e.g. Cox & Hinkley 1974) has been used to obtain the estimates and their errors. Briefly, the technique is as follows. Consider a set of n observations y_1, y_2, \dots, y_n used to obtain the estimate $\hat{\theta}_n(y_1, y_2, \dots, y_n)$ of some parameter θ . The parameter θ is again estimated but ignoring the observation y_j , then the estimator $\hat{\theta}_{-j}$ can be defined as

$$\hat{\theta}_{-j} = \hat{\theta}_{n-1}(y_1, y_2, \dots, y_{j-1}, y_{j+1}, \dots, y_n). \tag{14}$$

$\hat{\theta}_{-j}$ is computed for $j = 1, 2, \dots, n$ and the n pseudo-values $\hat{\theta}_{pj}, j = 1, 2, \dots, n$ defined by

$$\hat{\theta}_{pj} = n\hat{\theta}_n - (n-1)\hat{\theta}_{-j} \tag{15}$$

can be computed. The jack-knife estimator $(\hat{\theta}_n)^J$ is given by the average of the n pseudo-values and so

$$(\hat{\theta}_n)^J = \frac{1}{n} \sum_{j=1}^n \hat{\theta}_{pj}. \tag{16}$$

The bias of $(\hat{\theta}_n)^J$ is less than any bias the original estimator $\hat{\theta}_n(y_1, y_2, \dots, y_n)$ might have had an approximate confidence interval may be found for the parameter θ by treating

$$T = \frac{(\hat{\theta}_n)^J - \theta}{\sqrt{s^2}} \tag{17}$$

as a Student's t distributed variable on $(n-1)$ degrees of freedom where

$$s^2 = \frac{1}{n(n-1)} \sum_{j=1}^n \{\hat{\theta}_{pj} - (\hat{\theta}_n)^J\}^2. \tag{18}$$

The acceptability of the regression may be tested with the common chi-square test. If the regression has been performed on m observations then, under the null hypothesis that the model is correct, the sum of the weighted residuals will be a chi-square distributed variable on $(m-2)$ degrees of freedom. Thus if the sum of the weighted residuals does not exceed the critical value of the relevant chi-square distribution then there is no statistical reason for rejecting the null hypothesis.

6 Comparison of model with present field data

In Section 2 it was noted that an acceptable model for the latitude variation of PSV should not be inconsistent with the present field data. A least squares fit has been performed to the 1965 IGRF non-dipole field (from McElhinny & Merrill 1975) and this fit is presented in Fig. 5. The fit was performed with the constraint that $S_D = 0$ with the 'observations' (see Table 3) taken as the variances at 10° intervals in latitude. Because the measurement errors in this case will be much smaller than the variation with time, equal weight was given to each of these observations. From Fig. 5 it is immediately apparent that the model is not inconsistent with the present field data and that the shapes of the two curves differ in a systematic manner, as was suggested in Section 2 *should* be the case.

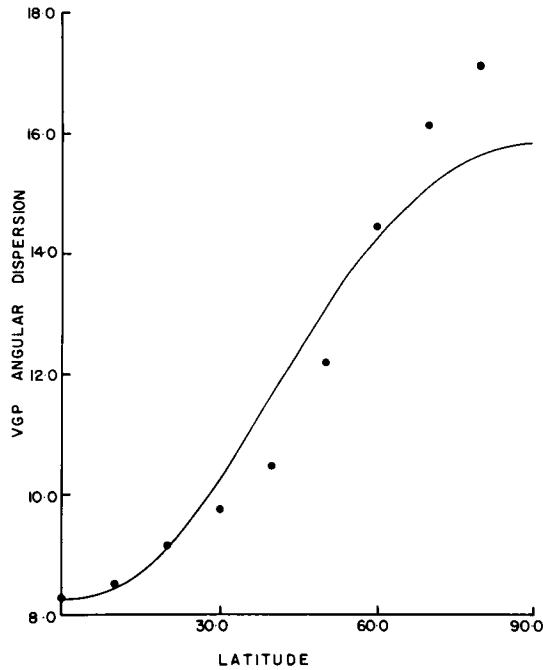


Figure 5. Least squares fit of model F to the 1965 IGRF non-dipole field.

7 Data selection

McElhinny & Merrill (1975) have outlined data selection methods for use in analysis of PSV. For the last 5 Myr it can be assumed that continental drift has been small and that all measured palaeodirections can be referred to the present axis of rotation. Lee & McElhinny (1984) have summarized a new data set for the past 5 Myr and these are summarized in Tables 4, 5 and 6. The analytical technique of McElhinny & Merrill (1975) has been used in which the VGPs are averaged over latitude bands. Separate analyses are given for normal (Table 4) and reversed (Table 5) data, but as Lee & McElhinny (1984) point out, incomplete demagnetization of rock samples tends to increase the dispersion of the reversed data and

Table 3. Angular dispersion of the 1965 IGRF non-dipole field.

Latitude	Dispersion (degrees)
0	8.25
10	8.50
20	9.16
30	9.74
40	10.48
50	12.21
60	14.44
70	16.17
80	17.16

Table 4. Normal polarity data for last 5 Ma.

Latitude Range	λ_m	N	s_f	s_L	s_U
0-15	2.7	361	12.0	11.4	12.7
15-25	19.8	394	13.7	13.1	14.4
25-30	27.7	226	14.8	13.9	15.8
30-40	36.7	146	15.3	14.2	16.7
40-50	45.4	160	16.9	15.7	18.3
50-60	55.7	103	17.1	15.6	19.0
>60	66.3	230	18.8	17.7	20.1

Notes

λ_m is the average latitude of the observations.
N is the number of observations in the latitude range.

s_f is the mean dispersion of VGPs in the latitude range and is the observed estimate of *S* in equation (1).

s_L and s_U are the lower and upper 95 per cent confidence limits for *S* within the latitude range.

All latitudes and dispersions are given in degrees.

Table 5. Reverse polarity data for last 5 Ma.

Latitude Range	λ_m	N	s_f	s_L	s_U
0-15	3.9	97	15.1	13.7	16.8
15-30	24.9	301	14.2	13.4	15.1
30-45	37.2	76	15.6	14.0	17.6
45-60	55.0	89	20.2	18.3	22.6
>60	64.9	199	20.6	19.3	22.2

For symbol definitions see Table 4.

Table 6. Combined polarity data for last 5 Ma.

Latitude Range	λ_m	N	s_f	s_L	s_U
0-15	2.9	458	12.7	12.2	13.3
15-25	20.1	541	13.4	12.9	14.0
25-30	28.0	380	15.1	14.4	15.9
30-40	36.7	211	15.5	14.5	16.6
40-50	45.1	188	16.7	15.6	18.0
50-60	56.4	175	19.0	17.7	20.5
>60	65.7	429	19.5	18.6	20.5

For symbol definitions see Table 4.

decrease that of the normal data. Combining the normal and reversed data tends to cancel out this effect (Table 6).

For data from rocks older than 5 Myr, continental drift must be taken into account. Euler rotations for the main continental plates are now known fairly precisely for the past 200 Myr. It is possible therefore to reconstruct the relative positions of the continents at

any time during this period. The palaeomagnetic data then determine the axis of rotation at any time. Lee & McElhinny (1984) have compiled data suitable for PSV in this way. At any point in time the departures of the VGPs from the calculated axis of rotation can be determined.

Because the data become very much fewer beyond 5 Myr, the VGP scatters can be accumulated over any length of time until sufficient data are available. A more detailed analysis of pre-5 Myr old data is given by Lee & McElhinny (1984) in terms of model F. In this paper the data are accumulated over three time spans 5–45, 45–110 and 110–195 Myr (Tables 8–10). Details are given by Lee & McElhinny (1984).

8 The last 5 Myr

Although it can be expected that separate normal and reverse PSV data will give lower and higher angular dispersions than expected respectively, a separate analysis has been carried out here to see if any differences can be determined. Best fitting parameter estimates are given in Table 7 and least square fits to the data are shown in Fig. 6. In both cases the model provides an acceptable fit to the data, although the fit to the normal polarity data is clearly better. This probably just reflects the fact that there are more data available for the normal field over the past 5 Myr. From the jack-knife results in Table 7, it is apparent that there is no discernible difference between the parameters for the normal polarity fit and those for the reversed polarity fit. The parameter estimates for the combined polarity fit are given in Table 7 and the least squares fit is shown in Fig. 7. The fit to these data is in fact very good with the probability that a chi-square distributed variable with five degrees of freedom will exceed 4.42 being 50 per cent.

Table 7. Parameter estimates for last 5 Ma.

<u>Least squares regression</u>									
	\hat{S}_D^2	$\text{Var}(\hat{S}_D^2)$	\hat{S}_D	\hat{S}_N^2	$\text{Var}(\hat{S}_N^2)$	\hat{S}_N	$\sigma_d(0)$	χ^2	$\chi^2_{0.95}$
Normal	56.5	176.9	7.5	100.8	86.0	10.0	14.70	9.33	11.07
Reverse	54.1	677.3	7.4	126.4	278.5	11.2	16.22	6.57	7.82
Combined	51.7	142.0	7.2	113.1	67.4	10.6	15.46	4.42	11.07
<u>Jack-knife results</u>									
	\hat{S}_D	$\text{Var}(\hat{S}_D)$	dof	95% limits	\hat{S}_N	$\text{Var}(\hat{S}_N)$	dof	95% limits	
Normal	7.3	5.15	6	1.7 < S_D < 12.8	10.2	1.26	6	7.5 < S_N < 13.0	
Reverse	5.8	13.21	4	0 < S_D < 15.9	12.2	1.72	4	8.5 < S_N < 15.8	
Combined	7.4	0.84	6	5.2 < S_D < 9.7	10.5	0.24	6	9.3 < S_N < 11.7	

Notes

\hat{S}_D^2 : estimate of S_D^2 .

$\text{Var}(\hat{S}_D^2)$: estimated variance of \hat{S}_D^2 from least squares.

\hat{S}_D : estimate of S_D (degrees).

\hat{S}_N^2 : estimate of S_N^2 .

$\text{Var}(\hat{S}_N^2)$: estimated variance of \hat{S}_N^2 from least squares.

\hat{S}_N : estimate of S_N (degrees).

χ^2 : value of chi-square test statistic.

$\chi^2_{0.95}$: critical value of chi-square distribution at 95 per cent level of confidence.

dof: degrees of freedom for Student's t distributed variable.

$\sigma_d(0)$: angular dispersion of field directions at equator (degrees).

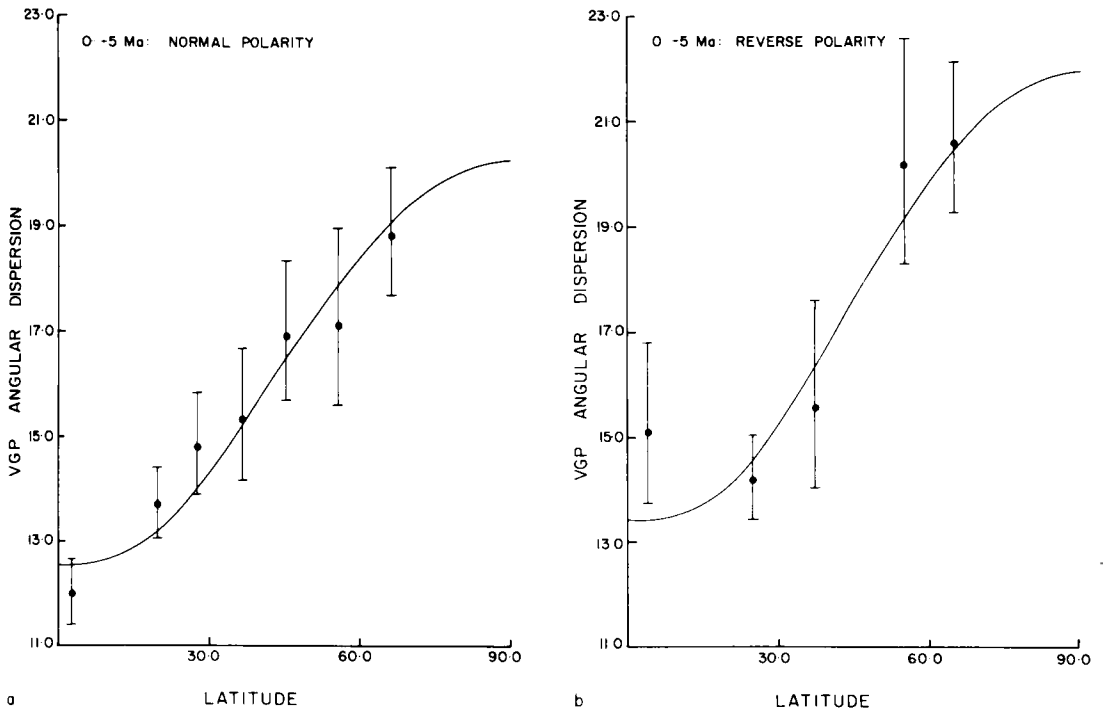


Figure 6. Least squares fit of model F to (a) normal and (b) reversed polarity data for the past 5 Myr.

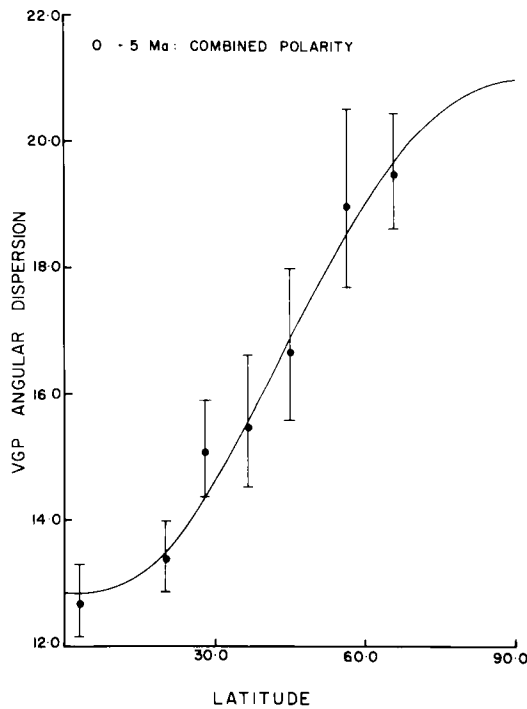


Figure 7. Least squares fit of model F to combined polarity data for the past 5 Myr.

8.1 COMPARISON WITH PREVIOUS VDM ANALYSIS

The fundamental relationship, equation (8), for the latitude variation of angular dispersion was derived assuming equation (3), this latter relation following from McFadden & McElhinny (1982). Estimation of the parameter S_N^2 is equivalent to estimation of the parameter k in (3). Similarly, it is possible to estimate the parameter k given the VDM analysis of McFadden & McElhinny (1982). A more meaningful parameter is $\sigma_d(0)$ which is given from (8) as

$$\sigma_d(0) = k\sqrt{2(1+a)/3} \quad (\text{rad}) \quad (19)$$

and this has already been estimated as part of the iterative least squares regression for the directional data. For purposes of comparison between the two studies $\sigma_d(0)$ will now be estimated from the results of the VDM analysis.

From the analysis of VDMs for the last 5 Myr McFadden & McElhinny (1982) were able to show that, to first order, the variance, $\sigma_{M_r}^2$, of VDMs caused by variations in the non-dipole components is given by

$$\sigma_{M_r}^2 = c^2 F^2 \quad (20)$$

with $c = 0.186$. In order to relate this to the dispersion of the directional data some distribution has to be assumed for $p_m(m|M)$. It is reasonable to assume that \mathbf{m} is caused by a large number of essentially independent variations and that the tip of \mathbf{m} therefore has a trivariate Gaussian distribution with some variance σ_m^2 . The variable m , which is just the length of \mathbf{m} , will therefore have the distribution $p_m(m|M)$ given by

$$p_m(m|M) dm = \frac{4m^2}{R^3\sqrt{\pi}} \exp(-m^2/R^2) dm \quad (21)$$

where

$$R = \sigma_m\sqrt{2} \quad (22)$$

is the mode (i.e. the most likely value) of m . This is in fact the distribution used by Cox (1970), and subsequent models, to determine the latitudinal variation of PSV. If θ is the angle between \mathbf{m} and \mathbf{M} then

$$M_r^2 = M^2 + m^2 + 2mM \cos \theta \quad (23)$$

and so for given m and M

$$\langle M_r \rangle = M + \frac{m^2}{3M}$$

$$\langle M_r^2 \rangle = M^2 + m^2 \quad (24)$$

$$\text{Var}(M_{r\theta}) = \langle M_r^2 \rangle - \langle M_r \rangle^2 = \frac{m^2}{3} \left(1 - \frac{m^2}{3M^2} \right).$$

As m varies the overall variance, $\sigma_{M_r}^2$, in the VDMs is given by

$$\begin{aligned} \sigma_{M_r}^2 &= \langle \text{Var}(M_{r\theta}) \rangle \\ &= \int_0^\infty \left(\frac{m^2}{3} - \frac{m^4}{9M^2} \right) \frac{4m^2}{R^3\sqrt{\pi}} \exp(-m^2/R^2) dm \\ &= \frac{1}{2}R^2 - \frac{5R^4}{12}. \end{aligned} \quad (25)$$

From (20) this must equal $c^2 M^2$ and so

$$c^2 M^2 = \frac{1}{2} R^2 - \frac{5 R^4}{12} \tag{26}$$

Letting

$$R = qM \tag{27}$$

then

$$c^2 = \frac{1}{2} q^2 - \frac{5}{12} q^4 \tag{28}$$

This suggests that as $p_f(f | F)$ the density given by

$$p_f(f | F) df = \frac{4 f^2}{R_f^3 \sqrt{\pi}} \exp(-f^2/R_f^2) df \tag{29}$$

can be used where R_f is the mode of f conditional upon F and

$$\langle f^2 | F \rangle = \frac{3}{2} R_f^2 \tag{30}$$

From (3) this gives

$$R_f = k\sqrt{(2/3)} F = qF \tag{31}$$

and since the distribution of directions does not have the spherical symmetry a function of the form

$$c^2 = uq^2 - wq^4 \tag{32}$$

can be used but u and w may not take on the values of $1/2$ and $(5/12)$ respectively as in (28).

Integrations over the directional distributions assuming the density of (29) have been performed numerically and it was found that for q in the range 0.0–0.6 the value of c is given to within 0.1 per cent by (32) with $u = 0.57483$ and $w = 0.12845$. The value of $c = 0.186$ determined by McFadden & McElhinny (1982) therefore gives $q = 0.2470$. Substitution of this result into (19) and interpolating the value of a from Table 1 gives

$$\sigma_d(0) = 15.39^\circ$$

This value of $\sigma_d(0)$ has been determined from the fit performed by McFadden & McElhinny (1982) to the VDM (i.e. intensity) data and agrees remarkably well with the value of $\sigma_d(0) = 15.46^\circ$ (see Table 6) obtained here by fitting to the directional data for the last 5 Myr.

It is important to know how sensitive this agreement is to the distribution assumed for f . To test this it was assumed that f could only take on a specific value R_f for each value of F with

$$R_f = qF \tag{33}$$

and

$$\langle f^2 | F \rangle = F^2 \tag{34}$$

Equation (3) then gives $k = q$ for this situation. Again it was found that with q in the range $0.0 \rightarrow 0.6$ an excellent fit is given by equation (32) but now with $u = 0.383278$ and $w = 0.135799$. The value of $c = 0.186$ then gives $q = 0.3055$ and substitution of this value into (19) gives

$$\sigma_f(0) = 15.54^\circ.$$

Clearly therefore the value of $\sigma_d(0)$ predicted from the intensity analysis is not at all sensitive to the density assumed for $P_f(f|F)$. The reason for this is that (3) is fundamental to the model and is essentially a statement regarding the average energy density in the non-dipole field and the energy density in the dipole field. Hence, no matter what distribution is chosen for f the fit is equivalent to balancing the energy densities and will give consistent values for $\sigma_d(0)$.

9 The period 5–195 Ma

Tables 8, 9 and 10 summarize the VGP angular dispersion data for the intervals 5–45, 45–110 and 110–195 Ma, from Lee & McElhinny (1984). Parameter estimates from model F for these three intervals are given in Table 11 and least squares fits are shown in Figs 8, 9 and 10.

Table 8. Combined polarity data 5–45 Ma.

Latitude Range	λ_m	N	s_f	s_L	s_U
0–15	10.9	110	18.6	17.0	20.6
15–30	23.8	274	17.6	16.6	18.7
30–45	43.3	293	21.6	20.4	22.9
45–60	50.3	527	20.1	19.3	21.0
>60	62.8	627	21.5	20.7	22.4

For symbol definitions see Table 4.

Table 9. Combined polarity data 45–110 Ma.

Latitude Range	λ_m	N	s_f	s_L	s_U
0–15	8.5	32	11.7	10.0	14.2
15–30	23.9	99	12.9	11.8	14.3
30–45	40.9	147	15.3	14.2	16.7
45–60	47.6	245	19.5	18.4	20.8
>60	64.3	25	20.9	17.4	26.1

For symbol definitions see Table 4.

Table 10. Combined polarity data 110–195 Ma.

Latitude Range	λ_m	N	s_f	s_L	s_U
0–20	11.1	69	18.5	16.6	21.0
30–40	34.3	66	18.5	16.5	21.1
>40	61.2	47	20.3	17.8	23.7

For symbol definitions see Table 4.

Table 11. Parameter estimates for 5–195 Ma, combined polarities.

Least squares regression

	\hat{S}_D^2	$\text{Var}(\hat{S}_D^2)$	\hat{S}_D	\hat{S}_N^2	$\text{Var}(\hat{S}_N^2)$	\hat{S}_N	$\sigma_d(0)$	χ^2	$\chi_{0.99}^2$
5–45 Ma	233.8	892.2	15.3	75.1	167.7	8.7	12.90	10.54	11.34
45–110 Ma	0	-----	0	151.6	43.3	12.3	17.52	11.90	13.28
110–195 Ma	299.0	4693	17.3	30.9	1182	5.6	8.56	0.22	6.64

Jack-knife results

	\hat{S}_D	$\text{Var}(\hat{S}_D)$	dof	95% limits	\hat{S}_N	$\text{Var}(\hat{S}_N)$	dof	95% limits
5–45 Ma	14.5	4.36	4	$8.7 < S_D < 20.3$	9.4	3.02	4	$4.6 < S_N < 14.2$
45–110 Ma	0	-----	—	-----	12.3	0.76	4	$9.9 < S_N < 14.7$
110–195 Ma	17.4	2.73	2	$10.3 < S_D < 24.5$	8.0	19.53	2	$0 < S_N < 27.1$

For symbol definitions see Table 6.

$\chi_{0.99}^2$: critical value of chi-square distribution at 99 per cent level of confidence.

It is unlikely that the parameters S_D^2 and S_N^2 remained constant over any of these periods of time and so the accumulated data within each latitudinal band are probably derived from a spread of these parameters. Consequently the 99 per cent level of confidence has been used as a rejection criterion for these fits rather than the 95 per cent level of confidence and, from Table 11, none of the fits may be rejected at this level of confidence.

The period 45–110 Ma is the most interesting in that it contains the Cretaceous Normal Polarity Interval. It was found that if an unconstrained least squares fit was performed the

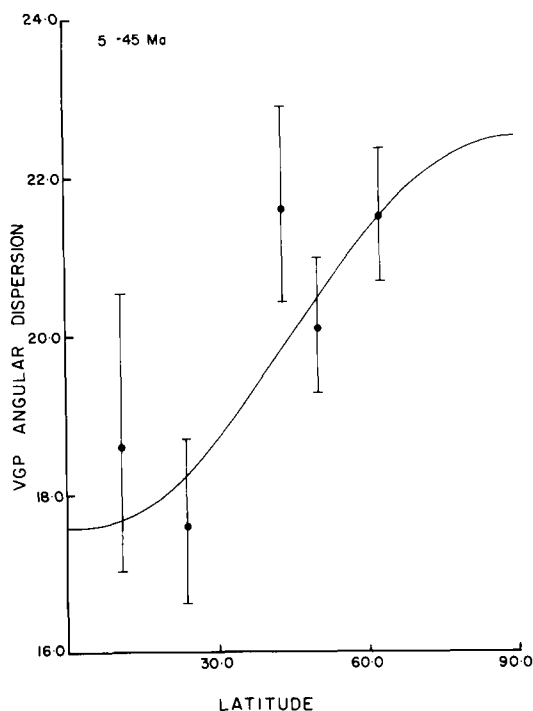


Figure 8. Least squares fit of model F to combined polarity data for the period 5–45 Ma.

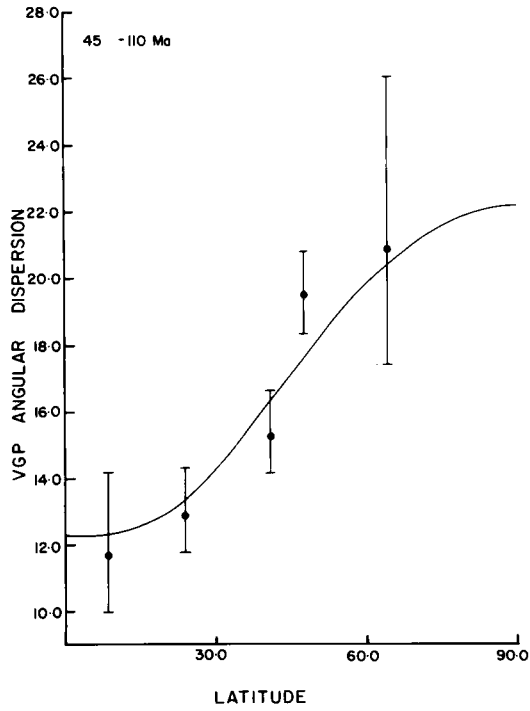


Figure 9. Least squares fit of model F to combined polarity data for the period 45–110 Ma.

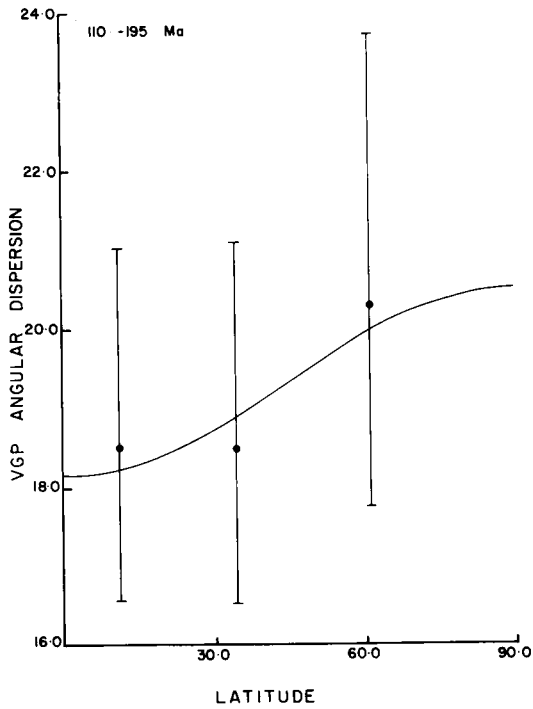


Figure 10. Least squares fit of model F to combined polarity data for the period 110–195 Ma.

estimated value of S_D^2 was negative – which is physically impossible. The only way to achieve a realistic fit was to constrain the model to having $S_D^2 = 0$.

From Fig. 10 it is immediately apparent that the data give very little information about S_N^2 during the period 110–195 Ma but do give some information about S_D^2 , the dipole wobble. This is confirmed by the errors given in Table 11.

10 Discussion

A simple model has been presented for the latitude variation in PSV which not only fits the palaeodata but also the data from the present field – an aspect which has eluded previous models. There are two fundamental differences between the present model and previous ones. Firstly, the effect on the latitude variation of the dispersion of directions caused by having spherically distributed VGPs rather than field directions has been taken into account – an effect which varies by a factor of more than $\sqrt{2}$ (in the dispersion) from equator to pole, yet has been ignored in previous models. Secondly, based on the intensity analysis of McFadden & McElhinny (1982), it is assumed that the average energy density of the non-dipole field has been linearly proportional to the energy density of the dipole field. An important consequence of this is that there is no need to assume a distribution for the intensity of either the non-dipole components or the dipole moment. This is a fundamental improvement over previous models.

Comparison of a statistical model fitted by McFadden & McElhinny (1982) to intensity data from the last 5 Myr with the present fit to directional data for the same period shows an excellent degree of consistency. The least squares fit to the directional data gives the angular dispersion of field directions at the equator as 15.4° and from the previous fit to the intensity data we would predict this dispersion to be about 15.5° – the precise value depending upon an assumed distribution for the intensity of the non-dipole components. The fit to the directional data gives the point estimate for k^2 as 0.0923 for the last 5 Myr. This implies that the average energy density in the non-dipole field at the surface of the Earth has been about 9 per cent of the energy density in the dipole field, this ratio being the controlling factor in the dispersion caused by variation in the non-dipole components. From Tables 7 and 11 it is apparent that the null hypothesis that S_N has remained constant from 195 Ma to the present cannot be rejected. If this is so then it is a remarkable feature. However, the results are not well constrained (particularly for the period 110–195 Ma) and so the inability to reject such an hypothesis is not, at this stage, very meaningful. In contrast the behaviour of S_D , the dipole wobble, is quite striking in that during the period 45–110 Ma it is necessary to set $S_D = 0$ to obtain a physically realistic fit. The implication is that the dipole wobble was zero (or at least very small) during the Cretaceous Normal Polarity Interval and the secular variation was due almost entirely to variation in the non-dipole components.

References

- Baag, C. & Helsley, C. E., 1974. Geomagnetic secular variation model E, *J. geophys. Res.*, **79**, 4918–4922.
- Barton, C. E. & McElhinny, M. W., 1981. A 10 000 yr geomagnetic secular variation record from three Australian maars, *Geophys. J. R. astr. Soc.*, **67**, 465–485.
- Cox, A., 1962. Analysis of present geomagnetic field for comparison with paleomagnetic results, *J. Geomagn. Geoelect.*, **13**, 101–112.
- Cox, A., 1968. Lengths of geomagnetic polarity intervals, *J. geophys. Res.*, **73**, 3247–3260.

- Cox, A., 1970. Latitude dependence of the angular dispersion of the geomagnetic field, *Geophys. J. R. astr. Soc.*, **20**, 253–269.
- Cox, A. & Doell, R. R., 1964. Long period variations of the geomagnetic field, *Bull. seism. Soc. Am.*, **54**, 2243–2270.
- Cox, D. R. & Hinkley, D. V., 1974. *Theoretical Statistics*, Chapman & Hall, London.
- Creer, K. M., 1962a. The dispersion of the geomagnetic field due to secular variation and its determination for remote times from paleomagnetic data, *J. geophys. Res.*, **67**, 3461–3476.
- Creer, K. M., 1962b. An analysis of the geomagnetic field using palaeomagnetic methods, *J. Geomagn. Geoelect.*, **13**, 113–119.
- Creer, K. M., Irving, E. & Nairn, A. E. M., 1959. Palaeomagnetism of the Great Whin Sill, *Geophys. J. R. astr. Soc.*, **2**, 306–323.
- Fisher, R. A., 1953. Dispersion on a sphere, *Proc. R. Soc. A*, **217**, 295–305.
- Harrison, C. G. A., 1980. Secular variation and excursions of the earth's magnetic field, *J. geophys. Res.*, **85**, 3511–3522.
- Irving, E., 1964. *Palaeomagnetism and its Application to Geological and Geophysical Problems*, Wiley, New York.
- Irving, E. & Ward, M. A., 1964. A statistical model of the geomagnetic field, *Pure appl. Geophys.*, **57**, 47–52.
- Kono, M., 1972. Mathematical models of the earth's magnetic field, *Phys. Earth planet. Int.*, **5**, 140–150.
- Lee, S. & McElhinny, M. W., 1984. Estimates of the time-variation of the non-dipole part of the time-averaged palaeomagnetic field, *Geophys. J. R. astr. Soc.*, submitted.
- McElhinny, M. W. & Merrill, R. T., 1975. Geomagnetic secular variation over the past 5 m.y., *Rev. Geophys. Space Phys.*, **13**, 687–708.
- McElhinny, M. W. & Senanayake, W. E., 1982. Variations in the geomagnetic dipole I: the past 50 000 years, *J. Geomagn. Geoelect.*, **34**, 39–51.
- McFadden, P. L. & McElhinny, M. W., 1982. Variations in the geomagnetic dipole 2: statistical analysis of VDMs for the past 5 million years, *J. Geomagn. Geoelect.*, **34**, 163–189.
- Roy, M. & Wagner, J. J., 1982. Palaeosecular variation and the current loop model of the geomagnetic field, *Geophys. J. R. astr. Soc.*, **71**, 269–273.
- Thompson, R. & Turner, G. M., 1979. British geomagnetic master curve 10 000–0 yr B.P. for dating European sediments, *Geophys. Res. Lett.*, **6**, 249–252.
- Zidarov, D. P. & Petrova, T. D., 1979. Presenting the earth magnetic field as a field of circular electric current loops, *C. r. Acad. bulg. Sci.*, **32**, 10–22.